Suppressing defect production during passage through a quantum critical point

Jay D. Sau[1] and K. Sengupta[2]
[1] *Condensed Matter Theory Center, University of Maryland, College Park, Maryland 20742, USA*
[2] *Theoretical Physics Department, Indian Association for the Cultivation of Science, Jadavpur, Kolkata-700032, India.*
(Dated: February 21, 2014)

We show that a closed quantum system driven through a quantum critical point with two rates ω_1 (which controls its proximity to the quantum critical point) and ω_2 (which controls the dispersion of the low-energy quasiparticles at the critical point) exhibits novel scaling laws for defect density n and residual energy Q. We demonstrate suppression of both n and Q with increasing ω_2 leading to an alternate route to achieving near-adiabaticity in a finite time for a quantum system during its passage through a critical point. We provide an exact solution for such dynamics with linear drive protocols applied to a class of integrable models, supplement this solution with scaling arguments applicable to generic many-body Hamiltonians, and discuss specific models and experimental systems where our theory may be tested.

PACS numbers: 73.43.Nq, 05.70.Jk, 64.60.Ht, 75.10.Jm

arXiv:1402.4805v1 [cond-mat.quant-gas] 19 Feb 2014

The physics of closed quantum systems driven out of equilibrium has received a lot of theoretical and experimental attention in recent years [1–3]. One of the central issues in this field involves understanding excitation or defect production in such a system upon its passage through a quantum critical point. It is well known when such a passage occurs due to a slow linear quench of a Hamiltonian parameter of the system characterized by a rate ω, the defect density n and the residual energy Q scale with universal powers $n \sim \omega^{d\nu/(z\nu+1)}$, $Q \sim \omega^{(d+z)\nu/(z\nu+1)}$, where d is the dimension of the system and z and ν are the dynamical critical and correlation length exponents[4, 5]. Such scaling laws can also be extended to cases where the system passes through a critical surface [6] and for non-linear ramps [7–9]. These scaling laws indicate an inevitable increase of n with increasing ω.

Such an increase of n and Q is disadvantageous for the purpose of quantum computation or dynamic preparation of a specific quantum state which necessitate implementation of dynamical protocols taking a quantum system from one ground state to another in a finite amount of time. Consequently, several theoretical suggestions for implementation of transitionless drive protocols have been put forth. A class of such protocols involve modification of the system Hamiltonian $H_0(t)$ by a suitably chosen $H_1(t)$ so that the instantaneous ground state of $H_0(t)$ becomes the exact solution of the many-body time dependent Schrodinger equation with $H(t) = H_0(t) + H_1(t)$[10, 11]. Such a procedure has been theoretically studied for several systems [10, 12–14]. However, its experimental implementation could be complicated; for example, for the transverse field Ising model [14], $H_1(t)$ involves several multispin non-local terms which might be difficult to implement in realistic experimental systems. Another route to such nearly transitionless dynamics involves use of optimal protocols as demonstrated for 1D Luttinger models in Ref. [15]. However, implementation of these protocols for arbitrary many-body systems remains a challenge.

In this letter, we provide an alternative route to suppression of defect density on passage through a quantum critical point. Our method involves driving two parameters of the generic Hamiltonian which reaches the critical point at $\lambda = \lambda_c \neq 0$ and has a quasiparticle dispersion $E_{\mathbf{k}} = c|\mathbf{k}|^z \equiv ck^z$ at the critical point. The first parameter driven according to the protocol $\lambda(t) = (\omega_1 t - \lambda_c)^\alpha$, where ω_1 is the rate and α is a positive exponent, controls the proximity of the system to the quantum critical point, while the second $c(t) = |\omega_2 t|^\beta$ controls the dispersion of the quasiparticles at the critical point. We show that under such a drive, for $\omega_1/\lambda_c^{\alpha z\nu+1} \ll 1$ and $\omega_2/\omega_1 \geq \omega_1^{\alpha\nu/[\beta(\alpha z\nu+1)]}/\lambda_c$, the defect density n scales as

$$n \sim \omega_1^{\left(\frac{\alpha\nu}{\alpha z\nu+1}+\frac{\beta}{z}\right)d}\omega_2^{-\beta d/z} \tag{1}$$

leading to its suppression with increasing ω_2. The scaling of Q is obtained by replacing $d \to (d+z)$ in Eq. 1 and shows an analogous suppression. We note that our results reproduce the standard single parameter scaling results of n and Q [4, 5, 7, 8] as a special case for $\beta = 0$ where $c(t)$ becomes a time independent constant. We provide an exact solution for a class of d-dimensional integrable models with linear ramp protocols ($\alpha = \beta = 1$) showing such behavior and supplement it with scaling arguments leading to Eq. 1 for arbitrary α and β. We also demonstrate a crossover between regimes where n and Q increases/decreases with increasing ω_1 and ω_2 with $\omega_2 = \omega_1^r$ ($r > 0$) and identity the exponent $r^* = 1+\alpha z\nu/[\beta(\alpha z\nu+1)]$ at which the crossover occurs. Finally, we discuss specific models and realistic experiments which could provide a test for our theory. We note that our results constitute a generalization of the well-known scaling laws for n and Q [4, 5, 7, 8]; in addition, they also provide a novel route to achieving near-adiabatic drive protocols for taking a quantum system through a critical point in finite time. We therefore expect our work to be of interest to theorists and experimentalists studying protocols of bit manipulations for quantum computation, dynamic preparation of quantum states, and non-equilibrium dynamics of strongly correlated quantum systems.

We begin by studying a class of d-dimensional integrable models with a Hamiltonian $H(t) = \sum_{\mathbf{k}} \psi_{\mathbf{k}}^\dagger H_{\mathbf{k}}(t)\psi_{\mathbf{k}}$, where $\psi_{\mathbf{k}} = (c_{1\mathbf{k}}, c_{2\mathbf{k}})$ are Fermionic operators and $H_{\mathbf{k}}(t)$ is given

by

$$H_{\mathbf{k}}(t) = \tau_3(\lambda_1(t) - b_{\mathbf{k}}) + \tau_1\lambda_2(t)g_{\mathbf{k}}. \quad (2)$$

Here τ_3 and τ_1 denote usual Pauli matrices while $b_{\mathbf{k}}$ and $g_{\mathbf{k}}$ are general functions of momenta. We shall first consider linear ramp protocol so that $\lambda(t) = \lambda_0\omega_1 t$ and $\lambda_2(t) = \lambda_0\omega_2 t$. In the rest of this work, we shall set $\hbar = 1$; all energy/frequency (time) units shall be understood to be in units of $\lambda_0(\lambda_0^{-1})$. The instantaneous eigenvalues of the Hamiltonian is given by $E_{\mathbf{k}}(t) = \pm\sqrt{(\lambda_1(t) - b_{\mathbf{k}})^2 + (\lambda_2(t)g_{\mathbf{k}})^2}$. The critical point is reached at $t = t_{0\mathbf{k}_0} = b_{\mathbf{k}_0}/\omega_1$ and $\mathbf{k} = \mathbf{k}_0$ where $g_{\mathbf{k}_0} = 0$ and $c(t) = |\lambda_2(t)|$ which reduces to $c(t_{\mathbf{k}_0}) = |\omega_2 b_{\mathbf{k}_0}/\omega_1|$ at the critical point. In what follows, we are going to assume that $b_{\mathbf{k}_0} \neq 0$ so that the critical point is reached at a finite $t_{0\mathbf{k}_0} \neq 0$, and $g_{\mathbf{k}} \sim |\mathbf{k} - \mathbf{k}_0| = k$ near the critical point.

To obtain a solution for the dynamics we note that the Hamiltonian density $H_{\mathbf{k}}(t)$ can be written in terms of a set of new Pauli matrices $\tilde{\tau}_3$ and $\tilde{\tau}_1$ as

$$H_{\mathbf{k}}(t) = \lambda_{1\mathbf{k}}(t - t_{1\mathbf{k}})\tilde{\tau}_3 + \lambda_{2\mathbf{k}}\tilde{\tau}_1, \quad (3)$$

where $t_{1\mathbf{k}} = b_{\mathbf{k}}\omega_1/\lambda_{1\mathbf{k}}$. In the above expression, the quantities $\lambda_{1\mathbf{k}}$ and $\lambda_{2\mathbf{k}}$ are given by

$$\begin{aligned} \lambda_{1\mathbf{k}} &= \sqrt{\omega_1^2 + \omega_2^2 g_{\mathbf{k}}^2} \\ \lambda_{2\mathbf{k}} &= \sqrt{(\omega_2 t_{1\mathbf{k}} - b_{\mathbf{k}})^2 + \omega_2^2 g_{\mathbf{k}}^2 t_{1\mathbf{k}}^2}, \end{aligned} \quad (4)$$

so that $t_{1\mathbf{k}_0} = t_{0\mathbf{k}_0}$ and the matrices $\tilde{\tau}_{1,3}$ can be expressed in terms of $\tau_{1,3}$ as

$$\begin{aligned} \lambda_{1\mathbf{k}}\tilde{\tau}_3 &= \omega_1\tau_3 + \omega_2 g_{\mathbf{k}}\tau_1, \\ \lambda_{2\mathbf{k}}\tilde{\tau}_1 &= (\omega_1 t_{1\mathbf{k}} - b_{\mathbf{k}})\tau_3 + \omega_2 t_{1\mathbf{k}} g_{\mathbf{k}}\tau_1 \end{aligned} \quad (5)$$

We note that the above transformation transfer the entire time dependence of $H_{\mathbf{k}}(t)$ to diagonal terms. From the structure of $H_{\mathbf{k}}(t)$ (Eq. 3), it is easy to see that the solution of the Schrodinger equation $i\partial_t\psi_{\mathbf{k}} = H_{\mathbf{k}}(t)\psi_{\mathbf{k}}$ amounts to solving a Landau-Zener problem for each $\mathbf{k}$ [16]. For a linear ramp protocol where the dynamics starts [ends] at $t \to -\infty[\infty]$, the probability of defect production for any $\mathbf{k}$ can be simply read off as [16, 17]

$$p_{\mathbf{k}} = e^{-\pi\lambda_{2\mathbf{k}}^2 g_{\mathbf{k}}^2/\lambda_{1\mathbf{k}}} = e^{-\pi\omega_2^2 b_{\mathbf{k}}^2 g_{\mathbf{k}}^2/(\omega_1^2+\omega_2^2 g_{\mathbf{k}}^2)^{3/2}} \quad (6)$$

which leads to the defect density and residual energies to be

$$n[Q] = \int d^dk/(2\pi)^d 1[E_{\mathbf{k}}] e^{-\pi\omega_2^2 b_{\mathbf{k}}^2 g_{\mathbf{k}}^2/(\omega_1^2+\omega_2^2 g_{\mathbf{k}}^2)^{3/2}}. \quad (7)$$

For $\omega_{1,2}/b_{\mathbf{k}_0}^2 \ll 1$ and $\omega_2/\omega_1 \geq \sqrt{\omega_1}/b_{\mathbf{k}_0}$, $p_{\mathbf{k}}$ is appreciable around $\mathbf{k} = \mathbf{k}_0$, where $b_{\mathbf{k}} = b_{\mathbf{k}_0}$ so that $p_{\mathbf{k}} = e^{-c\,\omega_2^2 k^2/\omega_1^3}$, with $c = \pi b_{\mathbf{k}_0}^2$. Substituting the expression for $p_{\mathbf{k}}$ in Eq. 7 and rescaling $k' = k\omega_2/\omega_1^{3/2}$, one obtains

$$n \sim \omega_1^{3d/2}\omega_2^{-d}, \quad Q \sim \omega_1^{3(d+1)/2}\omega_2^{-(d+1)}, \quad (8)$$

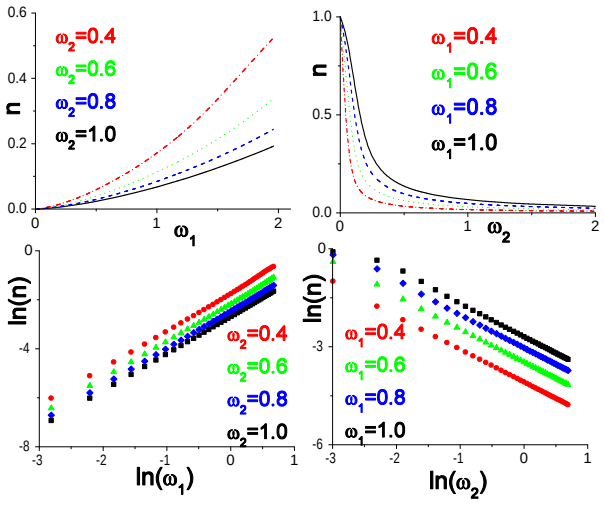

FIG. 1: (Color online) Top Panel: Plot of n vs ω_1 (left) and ω_2 (right) showing scaling of n. Bottom Panel: Plot of $\ln(n)$ as a function of $\ln(\omega_1)$ (left) and $\ln(\omega_2)$ (right). All plots are computed using Eq. 7 with $d = 1$, $b_{\mathbf{k}} = 5 - \cos(k)$, and $g(k) = \sin(k)$ so that H represents 1D XY model in a transverse field. The scaling regime, where Eq. 8 holds, occur for $\omega_2 \geq \omega_1^{3/2}/b_{\mathbf{k}_0} = 0.25\omega_1^{3/2}$.

where we have used the fact $E_{\mathbf{k}} \sim k$ around $\mathbf{k} = \mathbf{k}_0$. Note that the scaling relations allows for large values ω_2/ω_1; thus one can efficiently suppress defects by tuning ω_2 for a suitably chosen ω_1. A plot of n computed from Eq. 7 with $d = 1$, $b_{\mathbf{k}} = 5 - \cos(k)$, and $g_{\mathbf{k}} = \sin(k)$ (chosen so that the model conforms to 1D XY model in a transverse field) is shown in top panels of Fig. 1 as a function of the rates ω_1 and ω_2. The plot clearly demonstrates that n is a decreasing function of ω_2. In the scaling regime, the lines for different $\omega_2(\omega_1)$ in the bottom left(right) panels of Fig. 1 are parallel; their slope is numerically found to be $1.507(-0.994)$ which agrees well with the theoretically predicted values $3/2(-1)$.

From Eq. 8, we also expect that there are two separate regimes where the behavior of n is qualitatively different when both ω_1 and ω_2 is increased keeping $\omega_2 = \omega_1^r$ with $r \geq 0$. In the first[second] regime n increases[decreases] with ω_1 and ω_2. The crossover between these regimes occurs for $\omega_2 = \omega_1^{r^*}$ with $r^* = 3/2$ for any d. This crossover is indicated in Fig. 2, where n is plotted as function of ω_1 with $\omega_2 = \omega_1^r$. From the plot, we clearly find that n displays an increasing(decreasing) trend with ω_1 for $r < (>)r^*$. Interestingly, at $r = r^*$, n becomes independent of ω_1 and ω_2.

Next, we generalize Eq. 8 for non-linear ramps for which the exact solution no longer holds as follows. Consider a ramp for the Hamiltonian $H_{\mathbf{k}}(t)$ (Eq. 2) with $\lambda_1(t) = (\omega_1 t)^\alpha$ and $\lambda_2(t) = (\omega_2 t)^\beta$ where α and β are positive real numbers. Following Refs. [4, 18], we note that the system enters the impulse region where excitation production occurs around $t'_{0\mathbf{k}_0} = b_{\mathbf{k}_0}^{1/\alpha}/\omega_1$. Following Ref. [7], we linearize the Hamil-

tonian around $t = t'_{0\mathbf{k}_0}$ and $\mathbf{k} = \mathbf{k}_0$ to obtain

$$H_k^{\rm eff}(t) = \alpha b_{\mathbf{k}_0}^{(\alpha-1)/\alpha}\omega_1(t - t'_{0\mathbf{k}_0})\tau_3 + (\omega_2 t'_{0\mathbf{k}_0})^\beta k\tau_1. \quad (9)$$

The defect production for dynamics governed by $H_k^{\rm eff}(t)$ can be easily found; one can read off the off-diagonal element as $\Delta = (\omega_2 t'_{0\mathbf{k}_0})^\beta k = (\omega_2 b_{\mathbf{k}_0}^{1/\alpha}/\omega_1)^\beta k$ and $dE_{\mathbf{k}}(t)/dt \simeq \alpha b_{\mathbf{k}_0}^{(\alpha-1)/\alpha}\omega_1$. This allows one to obtain $p_{\mathbf{k}} \sim \exp[-\pi\Delta^2/|dE_{\mathbf{k}}(t)/dt|] \sim \exp[-\omega_2^{2\beta}\omega_1^{-(2\beta+1)}k^2]$ which leads to

$$n \sim \omega_1^{(2\beta+1)d/2}\omega_2^{-\beta d}, \quad Q \sim \omega_1^{(2\beta+1)(d+1)/2}\omega_2^{-\beta(d+1)}. \quad (10)$$

Note that Eq. 10 reproduces Eq. 8 for $\beta = 1$ and the standard one parameter drive scaling relations [4, 5, 7] for $\beta = 0$.

Eq. 10 can also be verified by a rigorous analysis. To this end, we note that the Schrodinger equation corresponding to the Hamiltonian given in Eq. 9 can be cast in the form of a Bloch equation

$$\partial_{t'}\boldsymbol{s} = \boldsymbol{B}(t') \times \boldsymbol{s}(t'), \quad (11)$$

where $\boldsymbol{B}(t') = [(\omega_2 t'/b_{\mathbf{k}})^\beta g_{\mathbf{k}}/b_{\mathbf{k}}, 0, (\omega_1 t'/b_{\mathbf{k}})^\alpha/b_{\mathbf{k}} - 1]$ is an effective magnetic field corresponding to the Hamiltonian $H_{\mathbf{k}}(t)$ (Eq. 2) and we have scaled $t' = b_{\mathbf{k}}t$. The spin variable $\boldsymbol{s}(t') = \langle\psi(t')|\boldsymbol{\tau}|\psi(t')\rangle$ in the Bloch equation characterizes the solution $|\psi(t')\rangle$ of the Schrodinger equation $i\partial_{t'}|\psi(t')\rangle = H_{\mathbf{k}}(t')|\psi(t')\rangle$ and $\boldsymbol{\tau} = \tau_1\hat{\boldsymbol{x}} + \tau_2\hat{\boldsymbol{y}} + \tau_3\hat{\boldsymbol{z}}$ is the vector of Pauli matrices. For future convenience, we introduce the rescaled frequencies $\tilde{\omega}_2 = \omega_2 g_{\mathbf{k}}^{1/\beta} b_{\mathbf{k}}^{-(1+\beta)/\beta}$ and $\tilde{\omega}_1 = \omega_1 b_{\mathbf{k}}^{-(1+\alpha)/\alpha}$; in terms of these rescaled frequencies, one can write

$$\boldsymbol{B}(t') = [(\tilde{\omega}_2 t')^\beta, 0, (\tilde{\omega}_1 t')^\alpha - 1]. \quad (12)$$

Next, we rewrite $\tilde{\omega}_2$ in terms of a new variable Γ so as to make the adiabatic limit $\tilde{\omega}_1 \to 0$ more transparent. To this end, the LZ impulse region occurs where $t' \sim 1/\tilde{\omega}_1$. In this region, the parameter which controls the transition probability is

$$\Gamma = \Big(|B(\tau)|^2/(2|\dot{B}(\tau)|)\Big)|_{\tau=\tilde{\omega}_1^{-1}} = \tilde{\omega}_2^{2\beta}/(2\alpha\tilde{\omega}_1^{1+2\beta}).$$

We will therefore parametrize $\tilde{\omega}_2$ as $\tilde{\omega}_2 = (2\alpha\tilde{\omega}_1{}^{1+2\beta}\Gamma)^{1/2\beta}$. The transition probability Φ, which is a function of $\tilde{\omega}_1, \tilde{\omega}_2$ is then more conveniently expressed as a function $\Phi(\tilde{\omega}_1, \Gamma)$ since it clearly reproduces the adiabatic limit where it is determined by Γ alone. In terms of this scaling function Φ, n can be written, as

$$n = \int_0^{\Lambda^{(0)}} \frac{d^d k}{2\pi}\Phi\Big(\omega_1 b_{\mathbf{k}}^{-(1+\alpha)/\alpha}, \frac{\omega_2^{2\beta} g_{\mathbf{k}}^2 b_{\mathbf{k}}^{(2\beta-\alpha+1)/\alpha}}{2\alpha\omega_1^{1+2\beta}}\Big),$$

where we have expressed Γ in terms of $\tilde{\omega}_2$ and $\Lambda^{(0)}$ represents the finite range of momentum integration that can be set of $\Lambda^{(0)} \to \infty$ in the scaling limit where $\omega_{1,2}/b_{\mathbf{k_0}}^{(1+\alpha)/\alpha} \ll 1$ and $\omega_2/\omega_1 \geq [\omega_1\alpha b_{\mathbf{k_0}}^{(\alpha-1)/\alpha}]^{1/(2\beta)}/b_{\mathbf{k_0}}^{1/\alpha}$ [19]. In the limit $\omega_1 \to 0$, the integral is dominated by $\mathbf{k} \sim \mathbf{k_0}$ such where $g_{\mathbf{k}} \sim k^z$ and $b_{\mathbf{k}} \to b_{\mathbf{k_0}}$. In this case, it is convenient to rescale the integration variable $k = [2\omega_1^{1+2\beta}\alpha k'/(\omega_2^{2\beta} b_{\mathbf{k_0}}^{(2\beta-\alpha+1)/\alpha})]^{1/2z}$ so that one can write [20]

$$n \sim \left(\frac{2\omega_1^{(1+2\beta)}\alpha}{\omega_2^{2\beta} b_{\mathbf{k_0}}^{(2\beta-\alpha+1)/\alpha}}\right)^{d/2z} \int_0^\infty \frac{dk'}{2z} k'^{\,d/2z-1}\Phi(0, k'), \quad (13)$$

which confirms the scaling relation (Eq. 10) for $z = 1$. A plot of $\ln(n)$ obtained by direct numerical solution of the Schrodinger equation corresponding to $H_{\mathbf{k}}(t)$ (Eq. 2) with $\lambda_1(t) = (\omega_1 t)^\alpha$ and $\lambda_2(t) = (\omega_2 t)^\beta$ as a function of $\ln(\omega_1)$ (left panel) and $\ln(\omega_2)$(right panel) for $d = z = 1$, $\alpha = 2$, $b_{\mathbf{k}} = 5 - \cos(k)$, and $g_{\mathbf{k}} = \sin(k)$ and several values of β, shown in Fig. 3, also confirms these scaling relations.

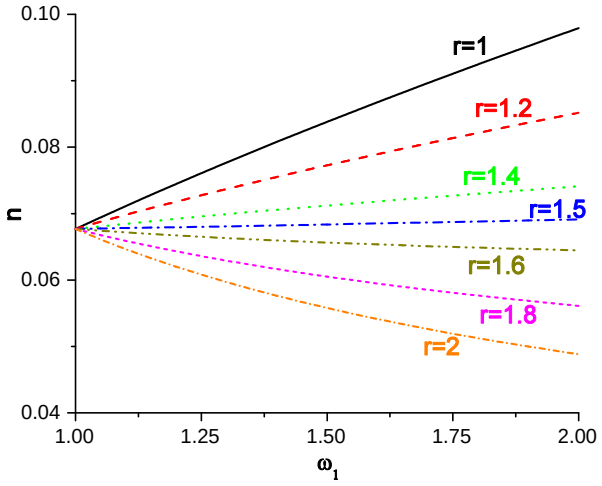

FIG. 2: Top panels: Plot of n vs ω_1 with $\omega_2 = \omega_1^r$ showing the crossover between regimes with increasing and decreasing n as a function of ω_1. All parameters are same as in Fig. 1.

Next, we provide a general system-independent scaling argument which leads to Eq. 1. We consider a generic Hamiltonian with two tunable parameters which are varied with rates ω_1 and ω_2. The first parameter $\lambda(t)$ controls the distance of the system from a quantum critical point at $\lambda = \lambda_c \neq 0$; for a generic Hamiltonian, this necessitates that the instantaneous energy gap near the critical point varies as $\Delta(\mathbf{k} = \mathbf{k}_0; \lambda) \simeq |\lambda(t)|^{z\nu} = |\omega_1 t - \lambda_c|^{z\nu\alpha}$, where α is a positive exponent and $\alpha = 1$ denotes linear drive protocol. The second parameter, $c(t)$, controls the dispersion of the quasiparticles at the critical point so that $\Delta(k, \lambda_c) \simeq c(t)k^z = |\omega_2 t|^\beta k^z$. Since the defect production occurs in the impulse region, which for small ω_1 is also the critical region, we first estimate the time spent by the system in this region. The Landau criterion for the system to be in the impulse region is given by [1] $d\Delta/dt \simeq \Delta^2$.

Substituting the expression for $\Delta(\mathbf{k}_0, \lambda(t))$ in this relation, one obtain an expression for T, the time spent by the system in the impulse region, as $|T - T_0| \simeq \omega_1^{-\alpha z\nu/(\alpha z\nu+1)}$, where $T_0 = \lambda_c/\omega_1$ is the time at which the system reaches the critical point. Substituting the expression for T in the expression for $\Delta(\mathbf{k}_0, \lambda)$, one finds that in the impulse region, the instantaneous energy gap behaves as

$$\Delta(\mathbf{k}_0; \lambda) \simeq \omega_1^{\alpha z\nu/(\alpha z\nu+1)} \tag{14}$$

which is in agreements with its counterpart for single parameter drive [1, 5, 7]. Next, we note that the defects or excitations are typically produced in a phase space $\Omega \sim k^d$ around the critical mode. For these modes, in the critical region, and during the time T that the system spends in this region, one has

$$\begin{aligned} k &\simeq |\omega_2 T_0|^{-\beta/z} \Delta(\mathbf{k}_0, \lambda(T))^{1/z} \\ &= |\omega_2 \lambda_c/\omega_1|^{-\beta/z} \Delta(\mathbf{k}_0, \lambda(T))^{1/z}. \end{aligned} \tag{15}$$

Using Eqs. 15 and 14, one finally gets

$$n \sim \Omega \simeq \omega_2^{-\beta d/z} \omega_1^{\left(\frac{\alpha\nu}{\alpha z\nu+1} + \frac{\beta}{z}\right)d}. \tag{16}$$

which reproduces the first relation in Eq. 1. We note that for the above arguments to hold we need near adiabatic dynamics which requites $\Delta(\mathbf{k}_0; T) \ll \Delta(\mathbf{k}_0; 0)$ in the impulse region leading to $\omega_1 \ll \lambda_c^{\alpha z\nu+1}$. Further, one also needs excitation production to occur at the neighborhood of $k \to 0$ which occurs when $(d\Delta(k, \lambda_c)/dk^z|_{t=T_0})^2 \geq d\Delta(\mathbf{k_0}; \lambda_c)/dt|_{t=T}$ and leads to the condition $\omega_2/\omega_1 \geq \omega_1^{\alpha\nu/[\beta(\alpha z\nu+1)]}/\lambda_c$. Also, the present analysis provides a general physical understanding of the defect suppression with increasing ω_2; it occurs due to the reduction of available momentum modes for quasiparticle excitations at any given energy $\Delta(k; \lambda)$ with increasing ω_2. Thus the role of the drive protocol changing $c(t)$ is to reduce the available phase space for defect production which naturally leads to suppression of n and Q with increasing ω_2. The expression for the residual energy Q can be similarly obtained by noting that the energy of the excitations produced for any k is given by $E[k] \simeq k^z$. This leads to $Q \sim k^z \Omega \sim k^{d+z} \sim \omega_2^{-\beta(d+z)/z} \omega_1^{\left(\frac{\alpha\nu}{\alpha z\nu+1} + \frac{\beta}{z}\right)(d+z)}$. From Eq. 1, we also find that the crossover between the regimes where n increases/decreases with ω_1 occurs for $\omega_2 = \omega_1^{r^*}$ with $r^* = 1 + \alpha z\nu/(\beta(\alpha z\nu + 1))$ which reduces to the condition $r^* = 3/2$ derived earlier for $\alpha = \beta = z = \nu = 1$.

Finally, we discuss concrete models where our theory shall hold. First we note that for $d = 1$, Eq. 2 represents the XY model in a transverse field with the identification: $b_{\mathbf{k}} = h_0 - \cos(k)$, $g_{\mathbf{k}} = \sin(k)$ $J_x[J_y] = 1/2[1 + (-)\omega_2 t]$ and $h(t) = \omega_1 t - h_0$. Our analysis leading to Eqs. 7 and 8 is therefore directly applicable to this model which has been extensively used in the past for test bed for Kibble-Zureck (KZ) scaling [1–3, 21]. Second, ultracold superfluid fermions with tunable zeeman field and spin-orbit coupling is another example where our scaling analysis is expected to be relevant. The

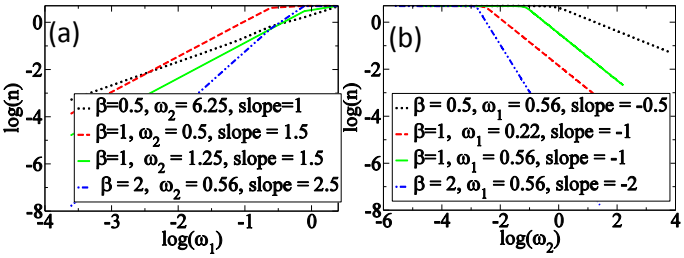
(a)
log(n)
log(ω1)
β=0.5, ω2= 6.25, slope=1
β=1, ω2 = 0.5, slope = 1.5
β=1, ω2 = 1.25, slope = 1.5
β = 2, ω2 = 0.56, slope = 2.5
(b)
log(n)
log(ω2)
β = 0.5, ω1 = 0.56, slope = -0.5
β=1, ω1 = 0.22, slope = -1
β=1, ω1 = 0.56, slope = -1
β = 2, ω1 = 0.56, slope = -2

FIG. 3: Color online: Plot of $\ln(n)n$ vs $\ln(\omega_1)$ (left panel) and $\ln(\omega_2)$ (right panel) showing slopes that are consistent with the theoretical exponents $(1 + 2\beta)d/(2z)$ and $-\beta d/z$ respectively (Eq. 13). All parameters are same as in Fig. 1. The exponent α does not appear to influence the slope and is taken to be 2. The frequencies $\omega_2(\omega_1)$ are held fixed as indicated in the left(right) panels.

effective Hamiltonians for such fermions is given by [22]

$$H_{\text{eff}} = \sum_{\mathbf{k}} \psi_{\mathbf{k}}^\dagger \left[\tau_z(v(t) - v_{zc}) + \tau_x \alpha(t) g(k)\right] \psi_{\mathbf{k}} \tag{17}$$

where $v(t) = \omega_1 t$ is the tunable zeeman field, $v_{zc} = \sqrt{\Delta_0^2 + \mu^2}$, Δ_0 is the superfluid order parameter, μ is chemical potential, $\alpha(t) = \omega_2 t$ is the amplitude of spin-orbit (Rashba) coupling, and $g(k) = \sin k$. The analysis leading to Eqs. 7 and 8 directly holds for this system. In addition, it has the advantage of being easily implementable using ultracold fermion systems. Finally, we note that almost all quantum systems near a phase transitions can be described a Landau-Ginzburg action which has the generic form

$$S = \int d^d r dt \psi^* [-\partial_t^2 + c_1 \sum_{i=1,d} \partial_{x_i}^{2z} + (r - r_c) - u|\psi|^2]\psi$$

Here r controls the distance to criticality while c_1 controls the quasiparticle dispersion at criticality. Our analysis holds for such theories if r and c_1 is tuned as functions of time with rates ω_1 and ω_2. These parameters are derivable, in principle, from the microscopic parameters of the system action; thus our method provides a generic algorithm for defect suppression by tuning microscopic parameters of a quantum system. We recognize that the precise experimental implementation, found to be simple for specific systems discussed above, could be difficult for generic actions (specially for strongly interacting systems where relation between microscopic tunable parameters and r, c_1 may be complicated); however, the present analysis at least serves as the first guideline in this respect.

In conclusion, we have obtained novel scaling laws for n and Q for a quantum system driven through a critical point with two rates ω_1 and ω_2 for arbitrary power law protocols. Our results constitute a generalization of KZ scaling to two parameter drive protocols. These results indicate suppression of both n and Q with increasing ω_2 and therefore provides a route to shortcut to adibaticity for driven quantum critical systems.

KS thanks D. Sen for discussions and S. Das Sarma for hospitality during early stages of this work. We also thank I. Spielman and F. Setiawan for discussions on a related work that motivated the present results. JS thanks the JQI/PFC, CMTC and the University of Maryland for start-up support.

SUPPLEMENTARY MATERIAL: SPIN ORBIT COUPLED COLD ATOMIC GASES

The Bogoliubov de-Gennes Hamiltonian for a spin-orbit coupled cold atomic fermi gas with attractive interactions is written as

$$H_{BdG,k}(t) = ((\epsilon_k - \mu(t) + \alpha(t)k\sigma_z)\tau_z + V_Z(t)\sigma_x + \Delta\tau_x, \tag{18}$$

where $\alpha(t)$ is the Rashba spin-orbit coupling, $V_Z(t)$ is the Zeeman splitting and $\mu(t)$ is the chemical potential. The dispersion $\epsilon_k = k^2$ where the effective mass has been set to $m = 0.5$ by an appropriate choice of units. In the experimental set-up involving artificial gauge fields [24], the Rashba spin-orbit parameter $\alpha(t)$ is set by the angle of the incident Raman beams and the Zeeman potential is controlled by the intensity of the Raman beams. The matrix $\sigma_{x,y,z}$ represent the spin degree of freedom, while the matrices $\tau_{x,y,z}$ represent the particle-hole degree of freedom.

In the adiabatic limit of slow frequency, transitions only occur near the critical gap closing point of the Hamiltonian $H_{BdG,k}(t)$ for t such that

$$\Delta^2 + \mu(t_c)^2 = V_Z(t_c)^2 \tag{19}$$

and near $k \approx 0$. Near the transition point, one can ignore the $\epsilon_k \sim k^2$ term and approximate the Hamiltonian as

$$H_{BdG,k}(t) \approx \alpha(t)k\sigma_z\tau_z + V_Z(t)\sigma_x + \Delta\tau_x - \mu(t)\tau_z. \tag{20}$$

Focusing on $k = 0$, we note that only one pair of eigenstates $|\pm\rangle$ of $H_{BdG,k=0}(t \sim t_c)$ are at energies of order $t \sim t_c$, while other pair are at energy $\sqrt{\Delta^2 + \mu(t_c)^2}$. Projecting at small k into these eigenstates

$$\begin{aligned} H_{BdG,k}(t) &\approx \alpha(t)k[|-\rangle\langle+|\langle+|\sigma_z\tau_z|-\rangle + h.c] \\ &+ [V_Z(t) - \sqrt{\Delta^2 + \mu(t)^2}][|+\rangle\langle+| - |-\rangle\langle-|]. \end{aligned} \tag{21}$$

Defining a pseudo-spin $\rho_x = |+\rangle\langle-| + h.c$ and $\rho_z = [|+\rangle\langle+| - |-\rangle\langle-|]$, we can write the effective Hamiltonian as

$$\begin{aligned} H_{BdG,k}(t) &\approx k\alpha(t)\frac{\Delta}{\sqrt{\Delta^2 + \mu(t)^2}}\rho_x \\ &+ [V_Z(t) - \sqrt{\Delta^2 + \mu(t)^2}]\rho_z. \end{aligned} \tag{22}$$

The chemical potential $\mu(t)$ in a closed system should be set by the density. In the limit of small $\Delta, V_Z(t), \mu(t) \ll \alpha(t)$, one can ignore the time-dependence of $\mu(t)$ and approximate $\mu(t) \approx 0$. This leads to

$$H_{BdG,k}(t) \approx k\alpha(t)\rho_x + [V_Z(t) - \Delta]\rho_z. \tag{23}$$

Choosing appropriate time-dependence for $\alpha(t)$ and $V_Z(t)$ leads to the model (Eq. [17] in the main text) discussed in the main text.

[1] A. Polkovnikov, K. Sengupta, A. Silva, and M. Vengalattore, Rev. Mod. Phys., **83**, 863 (2011).
[2] J. Dziarmaga, Adv. Phys. **59**, 1063 (2010).
[3] A. Dutta, U. Divakaran, D. Sen, B. K. Chakrabarti, T. F. Rosenbaum, and G. Aeppli, arXiv:1012.0653 (unpublished).
[4] T. W. B. Kibble, J. Phys. A **9**, 1387 (1976); W. H. Zurek, Nature (London) **317**, 505 (1985).
[5] A. Polkovnikov, Phys. Rev. B **72**, 161201(R) (2005).
[6] K. Sengupta, D. Sen and S. Mondal, Phys. Rev. Lett. **100**, 077204 (2008).
[7] D. Sen, K. Sengupta and S. Mondal, Phys. Rev. Lett. **101**, 016806 (2008).
[8] A. Polkovnikov, Phys. Rev. Lett. **101**, 220402 (2008).
[9] A. Chandran, A. Erez, S. S. Gubser, and S. L. Sondhi, Phys. Rev. B **86**, 064304 (2012).
[10] M. V. Berry, J. Phys. A: Math. Theor. **42**, 365303 (2009).
[11] M. Demirplak and S. A. Rice, J. Chem. Phys. A **107**, 9937 (2003); *ibid*, J. Chem. Phys. B **109**, 6838 (2005).
[12] B. Julia-Daz, E. Torrontegui, J. Martorell, J. G. Muga, and A. Polls, arXiv:1207:1483 (unpublished).
[13] B. Julia-Daz, T. Zibold, M. K. Oberthaler, M. Mele-Messeguer, J. Martorell, and A. Polls, arXiv:1205.6756 (unpublished).
[14] A. del Campfo, M. Rams, and W.H. Zurek, Phys. Rev. Lett. **109**, 115703 (2012).
[15] A. Rahmani and C. Chamon Phys. Rev. Lett. **107**, 016402 (2011).
[16] L.D. Landau, Phys. Z. Sowjetunion **2**, 46 (1932); G. Zener, Proc. R. Soc. London, Ser. A **137**, 696 (1932).
[17] N. V. Vitanov and B. M. Garraway, Phys. Rev. A **53**, 4288 (1996).
[18] B. Damski Phys. Rev. Lett. **95**, 035701 (2005).
[19] For $\omega_2 \to 0$, the integral diverges and needs to be regulated by an ultraviolet cutoff. However, this is irrelevant in the scaling regime; note that the conditions for the scaling regimes reduce to those for Eq. 7 for $\alpha = \beta = 1$.
[20] Here we have used the fact that $\omega_1/b_{\mathbf{k_0}}^{(\alpha+1)/\alpha} \to 0$ and used the fact the angular part of the integration is an irrelevant constant in the scaling regime where Φ depends only on k.
[21] V. Mukherjee Euro. Phys. Lett. **92**, 37004 (2010).
[22] For details of this derivation, see supplementary materials.
[23] L. Jiang, T. Kitagawa, J. Alicea, A. R. Akhmerov, D. Pekker, G. Refael, J. I. Cirac, E. Demler, M. D. Lukin, P. Zoller, Phys. Rev. Lett. **106**, 220402 (2011)
[24] Y-J. Lin *et al.* Nature (London) **471**, 83 (2011).